Hindawi Publishing Corporation
Journal of Nanomaterials
Volume 2013, Article ID 413692, 8 pages
http://dx.doi.org/10.1155/2013/413692

Research Article

Synthesis and Characterization of Stable and Binder-Free Electrodes of TiO_2 Nanofibers for Li-Ion Batteries

Phontip Tammawat[1] and Nonglak Meethong[2,3]

[1] *Materials Science and Nanotechnology Program, Faculty of Science, Khon Kaen University, Khon Kaen 40002, Thailand*
[2] *Department of Physics, Faculty of Science, Khon Kaen University, Khon Kaen 40002, Thailand*
[3] *Nanotec-KKU Center of Excellence on Advanced Nanomaterials for Energy Production and Storage, Khon Kaen 40002, Thailand*

Correspondence should be addressed to Nonglak Meethong; nonmee@kku.ac.th

Received 14 March 2013; Accepted 14 April 2013

Academic Editor: Mojtaba Samiee

An electrospinning technique was used to fabricate TiO_2 nanofibers for use as binder-free electrodes for lithium-ion batteries. The as-electrospun nanofibers were calcined at 400–1,000°C and characterized using X-ray diffraction (XRD), scanning electron microscopy (SEM), and transmission electron microscopy (TEM). SEM and TEM images showed that the fibers have an average diameter of ~100 nm and are composed of nanocrystallites and grains, which grow in size as the calcination temperature increases. The electrochemical properties of the nanofibers were evaluated using galvanostatic cycling and electrochemical impedance spectroscopy. The TiO_2 nanofibers calcined at 400°C showed higher electronic conductivity, higher discharge capacity, and better cycling performance than the nanofibers calcined at 600, 800, and 1,000°C. The TiO_2 nanofibers calcined at 400°C delivered an initial reversible capacity of 325 $mAh{\cdot}g^{-1}$ approaching their theoretical value at 0.1 C rate and over 175 $mAh{\cdot}g^{-1}$ at 0.3 C rate with limited capacity fading and Coulombic efficiency between 96 and 100%.

1. Introduction

Rechargeable lithium-ion batteries are among the most advanced electrical energy storage systems available today. Lithium-ion batteries have many notable advantages, particularly their higher volumetric and gravimetric energy densities, when compared with competing battery technologies. These features allow for lighter and smaller battery packs, a long cycle life, and a high-power rate. Nanomaterials also have many advantages, such as a higher surface-to-volume ratio and a shorter path length. Consequently, they have been used in energy storage technology to improve many material properties, leading to materials with high surface reactivity and high carrier transport.

Titanium dioxide (TiO_2) is one of the most promising candidates for use as an anode material in lithium-ion batteries due to its relatively high charge-discharge potential compared to graphite, high energy density, low cost, and environmental friendliness [1–3]. However, like many ceramic battery materials, such as $LiFePO_4$ [4], TiO_2 has an intrinsically low Li-ion diffusivity and a low electronic conductivity [5], diminishing its potential for applications in lithium-ion batteries. One approach to resolving this problem and increasing the rate performance of TiO_2 is to fabricate TiO_2 in a one-dimensional nanostructured form. Nanowires [6], nanotubes [7, 8], and nanoribbons [8] of TiO_2 have been studied and reported to demonstrate good performance due to their higher electrode/electrolyte contact area and shorter transport path lengths for electrons and Li-ions.

In this work, the structural, morphological, and electrochemical properties of TiO_2 nanofibers, another one-dimensional nanostructured form of TiO_2, with different anatase to rutile ratios were studied. An electrospinning technique was chosen to prepare the nanofibers due to its low cost and simple setup characteristics. In practice, this method

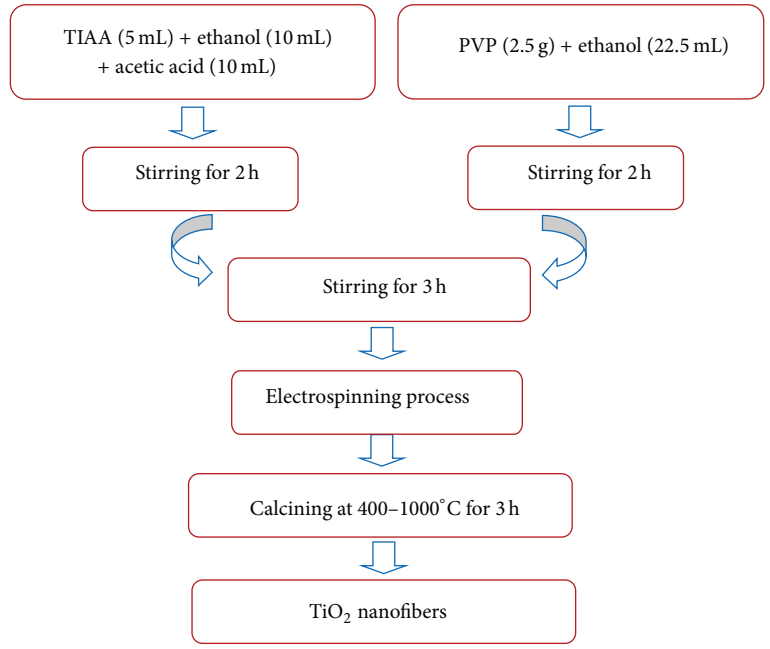

FIGURE 1: Synthesis procedure of TiO_2 nanofibers via electrospinning and calcination at 400–1,000°C in air for 3 hrs.

may facilitate the scale-up and mass production of the electrodes for Li-ion batteries without the need of various steps in the conventional process such as mixing (of active materials with conductive additives and binders), casting, vacuum drying, and slitting. This technique can be used to fabricate nanofibers that are exceptionally long and uniform in diameter and that have various compositions.

Much research effort has been focused on the potential applications of electrospun TiO_2 nanofibers for Li-ion batteries [8–11]. However, we found that this earlier work reported electrochemical testing of nanofibers using conventional composite electrodes. To ensure that the nanofibers are well mixed with a carbon additive and a binder, substantial grinding and mixing steps are required. Our objective in this work is to report the results obtained by using TiO_2 nanofibers as electrode materials for Li-ion batteries directly rather than making conventional composite electrodes. The electrodes contain almost 100 wt% active material. Typical electrodes contain 80 wt% active material and 20 wt% conductive and binder additives. Here, we hope to employ the unique properties of highly crystalline, long, and 3D porous nanofibers without a polymer binder and a conductive additive so that we can evaluate the potential of nanofibers for use as binder-free electrodes for Li-ion batteries. TiO_2 can be produced in various polymorphs such as anatase, rutile, and brookite. However, TiO_2 in its anatase form is considered the most electroactive Li-insertion host among these polymorphs [12]. Therefore, previous studies focused on the electrochemical properties of the anatase structure. In this work, the electrochemical properties of rutile phase also were studied. Producing nanofibered TiO_2 from various ratios of anatase to rutile phases has not been previously reported.

2. Experimental

2.1. Preparation of TiO_2 Nanofibers. The electrospun TiO_2 nanofibers were prepared from precursors containing titanium (diisopropoxide) bis(2, 4-pentanedionate) 75 wt.% in 2propanol (TIAA), polyvinylpyrrolidone (PVP, M_n = 1,300,000), acetic acid, and ethanol. The preparation procedure of these nanofibers is shown in Figure 1. First, 5 mL of TIAA was dissolved in 10 mL ethanol and 10 mL acetic acid. Then, 2.5 g of PVP was dissolved in 22.5 mL ethanol. Both solutions were mixed using a magnetic stirrer at room temperature to form a viscous solution for electrospinning. The solution is loaded into a plastic syringe pump with a needle. The electrospinning system was subjected to a voltage of 15 kV. The solution was fed at a rate of 1 mL/h, and the as-electrospun nanofibers were calcined in air at 400–1,000°C for 3 hrs.

2.2. Characterization of TiO_2 Nanofibers. The crystalline phases were identified using X-ray diffraction (PW3710 MPD Control Systems, the Netherlands) with Cu K_α radiation (λ = 0.15406 nm). The morphology of the nanofibers was observed using scanning electron microscopy (SEM; LEO 1450 VP, Cambridge, UK) and transmission electron microscopy (TEM; FEI Tecnai G2 20, Oregon, USA). Microanalysis of carbon content was performed using a LECO CHNS-932 elemental analyzer (LECO Corp., USA).

2.3. Preparation of Electrochemical Cells. The electrochemical performance of the fibers was studied using a square piece of ~3 mg·cm^{-2} of the TiO_2 nanofibers without adding a binder or conductive carbon. Li-metal foil was utilized

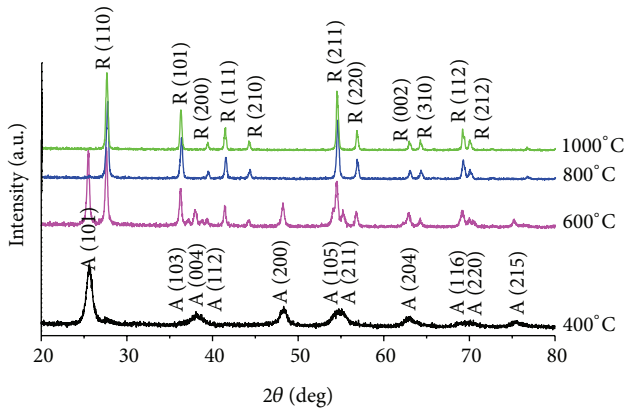

FIGURE 2: XRD patterns of nanofibers calcined at different temperatures.

as the anode and the reference electrodes. The electrolyte was created by dissolving 1 M $LiPF_6$ in a 1 : 1 (v/v) mixture of ethylene carbonate and diethyl carbonate. A microporous polymer (Celgard 2400) was used as the separator. When assembling the electrode, the Li foil was placed on inside of the Swagelok parts, and then the polymer separator was placed on the top. The calcined nanofiber piece was placed on top of the separator, and the electrolyte then added. A Cu disk was finally placed directly on top of the soaked nanofibers. The assembly process was done in an Ar-gas filled glove box. The cells were galvanostatically charged and discharged at 30°C over a voltage range of 0.5–3.0 V versus Li^+/Li using a battery cycler constructed from National Instruments (Austin, TX, USA) modular electronic components. The battery cycle was operated by a computer using LabVIEW software. Several electrochemical cells made out of the same batch of the fibers have also been tested using a commercial electrochemical tester (Gamry REF 3000, PA, USA) for the system's accuracy and yielded indistinguishable results (not shown). Electrochemical impedance spectroscopy (EIS) was performed over a frequency range of 0.1 to 10^6 Hz with an applied amplitude of 5 mV (Gamry REF 3000, PA, USA).

3. Results and Discussion

3.1. Structural Characterization of TiO_2 Nanofibers. X-ray diffraction analysis (shown in Figure 2) shows that the nanofibers consist of TiO_2 crystallites in the form of either anatase, rutile, or mixed anatase-rutile phase depending on the calcination temperature.

The nanofibers calcined at 400°C showed pure anatase phase. The nanofibers calcined at 800 and 1,000°C were composed of highly pure rutile phase, whereas the nanofibers calcined at 600°C consist of mixed anatase-rutile phase. The ratio between the rutile and anatase phases extracted from the XRD spectrum was calculated using the Spurr equation [13]

$$F_R = \frac{1}{1 + 1.26\left[I_A(101)/I_R(110)\right]}, \quad (1)$$

where F_R is the percentage content of the rutile phase and $I_A(101)$ and $I_R(110)$ are the integral intensities of the anatase and rutile phases, respectively. The ratio of rutile to anatase for the nanofibers calcined at 600°C was calculated to be 45%.

Figures 3 and 4 show SEM images and corresponding calculated particle size distribution of the as-spun and calcined nanofibers. The average diameter of the as-spun TiO_2/PVP composite nanofibers was approximately 160–200 nm. The diameter of the nanofibers calcined at 400–800°C was approximately 100–120 nm.

The reduction in size of the nanofibers after calcination was attributed to the loss of PVP from the nanofibers. It is believed that the PVP is decomposed to form amorphous carbon in air at 300°C [14]. A microanalysis of carbon content performed using a LECO CHNS-932 elemental analyzer shows that the nanofibers calcined at 400°C–1000°C in this study contained approximately 0.35, 0.09, 0.14, and 0.74 weight percent (wt%), respectively. After calcination at 800°C, the morphology of the nanofibers was changed, exhibiting connected particles rather than continuous fibers. Figure 3(e) shows an SEM image of the samples calcined at 1000°C. The samples appear to consist of linked particles with sizes ranging from 100 to 200 nm and have the same diameter as the fibers. These changes in morphology are related to a drastic change in crystal structure from anatase to rutile, as observed in other electrospun fibers such as vanadium pentoxide (V_2O_5) [15], sodium cobalt spinel ($NaCo_2O_4$) [16], and barium strontium titanate [17].

TEM images (Figure 5) show the morphology of the nanofibers at higher magnification. As shown, the nanofibers are composed of nanocrystallites ranging from 5–10 nm in size for the samples calcined at 400°C to 50–70 nm for the nanofibers calcined at 600°C and 50–200 nm for the fibers calcined at 800°C. The grain size of the fibers calcined at 1,000°C was approximately 100–300 nm. The primary crystallites of the nanofibers calcined at 400°C appear to be well connected.

3.2. Electrochemical Properties of TiO_2 Nanofibers. Electrochemical impedance spectroscopy (EIS) technique can be used to study electronic conductivity of the nanofibers. Figure 6 shows the characteristic shape of a Nyquist plot, with a semicircle in the high-frequency region connected by a straight line to the low-frequency region. The semicircle in the high-frequency region corresponds to charge-transfer resistance at the electrode/electrolyte interface. The straight line at low frequencies represents a solid-state diffusion-controlled process of Li-ions [18]. Here, we can see that the charge-transfer resistance of the nanofibers having anatase structure is smaller than that of the samples containing rutile phase. This lower charge-transfer resistance suggests better electron and lithium-ion transport kinetics and is responsible for the better electrochemical performance of the nanofibers with anatase structure.

The electrochemical performance of the nanofibers calcined at 400–1000°C, which featured polymorphs of pure anatase, mixed rutile and anatase, and pure rutile, was

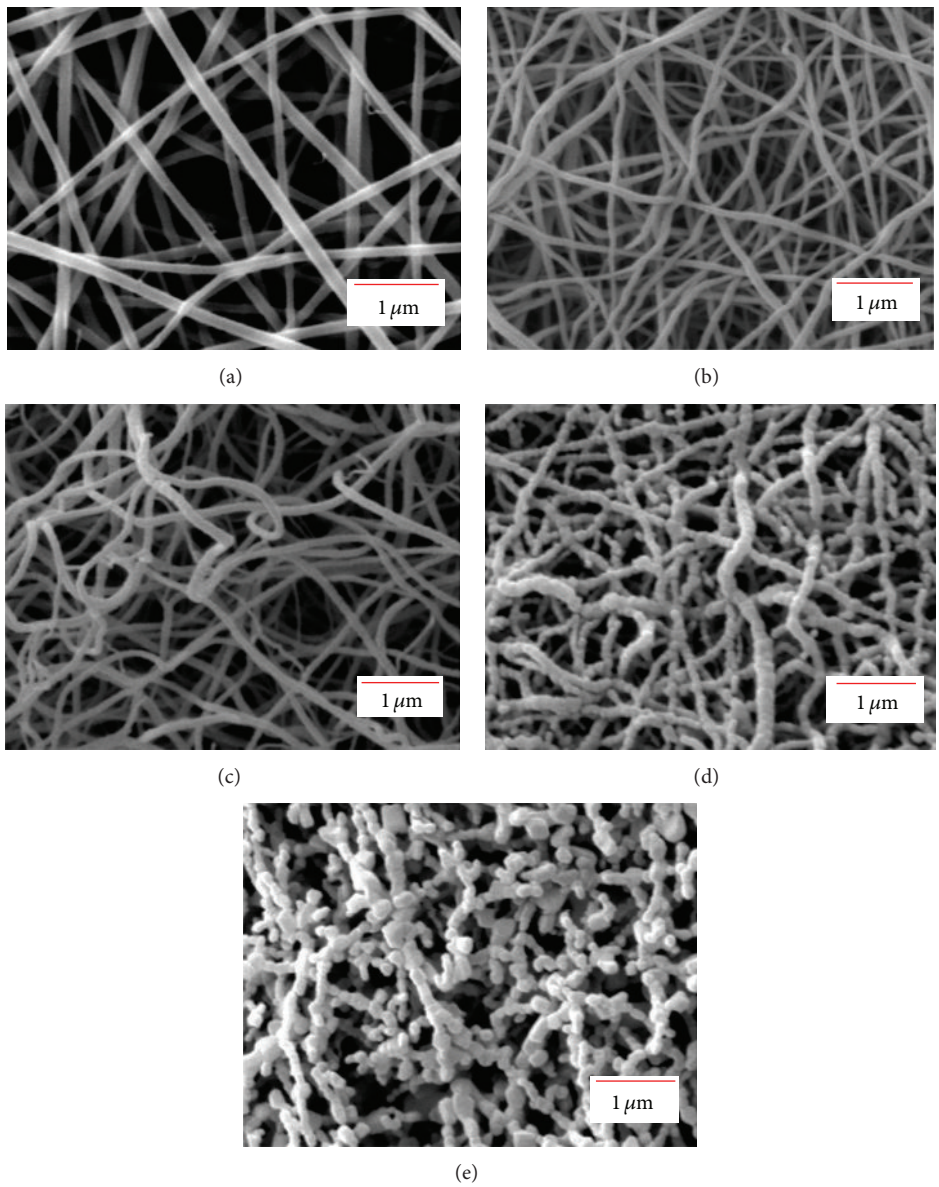

Figure 3: SEM images of TiO_2 nanofibers. (a) As-spun nanofibers. (b)–(e) Fibers calcined in air for 3 h at 400, 600, 800, and 1,000°C, respectively.

evaluated. Figure 7 shows charge-discharge profiles for the first few cycles of the nanofibers at 0.1 C (0.1 C means that it takes 10 hrs to fully charge this electrode to the cutoff voltage) assuming a theoretical capacity of 335 $mAhg^{-1}$. As seen, the discharge capacity of the samples calcined at 800–1000°C is lower than those of the samples calcined at 400°C and 600°C. This result shows that the rutile phase in the nanofibrous form of TiO_2 is also less electrochemically active than the anatase form. For the nanofibers calcined at 400°C, the low C-rate discharge capacity is very high and approaches its theoretical value. The effect of crystallite size is also evident. It can be seen that when the crystallite size decreases, the electrochemical performance is enhanced. The special properties of these nanostructures, that is, their high surface-to-volume ratio and short lithium diffusion path length with high electronic conductivity, are likely responsible for this observed result. The effects of particle size on enhancing electrochemical performance of battery electrodes have also been observed in other battery materials such as $Li_4Ti_5O_{12}$ titanate anodes [19] and $LiFePO_4$ olivine cathodes [20].

Voltage plateaus at 1.78 V and 1.90 V are observed in the discharge and charge curves, respectively. This finding is related to the phase transformation from-to Li_xTiO_2 (anatase, $I4_1/amd$) to-from Li_yTiO_2 (orthorhombic distortion, *Imma*) during cycling, where Li_xTiO_2 and Li_yTiO_2 represent the Li-poor and Li-rich phases of this compound, respectively [21]. The nanofibers calcined at 400°C exhibit the largest plateau region, followed by the fibers calcined at 600, 800, and 1000°C, respectively. Another interesting feature appears at the beginning of the charge and discharge processes

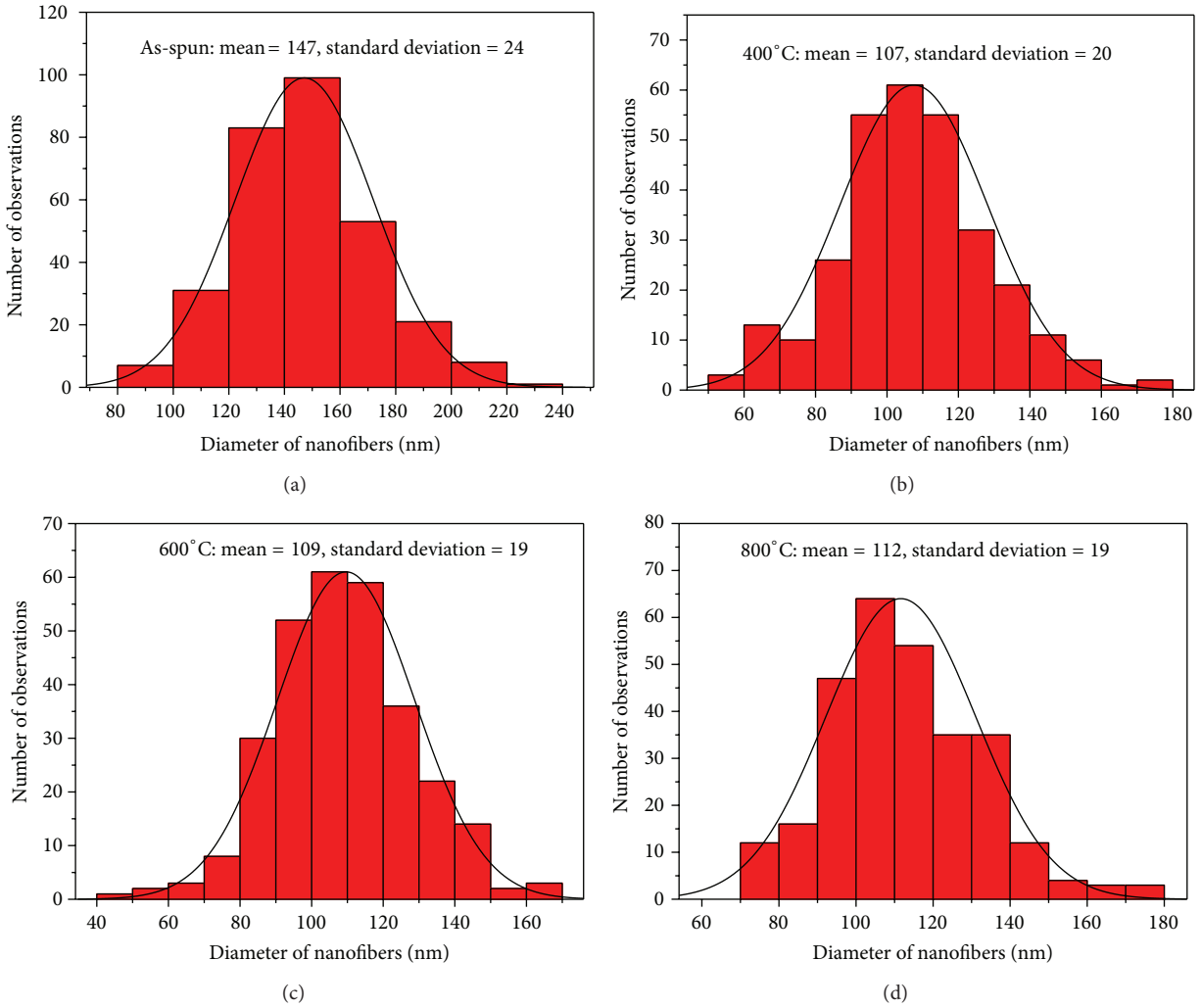

FIGURE 4: The calculated particle size distribution of the TiO_2 nanofibers. (a) As-spun nanofibers. (b)–(d) Fibers calcined in air for 3 h at 400, 600, 800, and 1,000°C, respectively.

of the samples containing different polymorphs. The samples containing the rutile phase show similar voltage profiles, with very similar values of x and y, regardless of the particle size. The nanofibers containing pure anatase phase (calcined at 400°C) show much larger x and y values. This result is interesting and may explain why the anatase form is more electrochemically active than the rutile form. The extended nonstoichiometric behavior in lithium-rich and lithium-poor phases has been correlated to the enhanced rate capability of olivine cathode material as well [22]. As has been established, a transformation related to a topotactic insertion mechanism is much faster than that related to the two-phase transformation mechanism. Hence, samples with large values of x and y should exhibit enhanced electrochemical performance.

Figure 8 shows the rate performance and cyclic stability of the nanofibers with pure anatase structure. Each data point is calculated from the average of three electrodes. The data points for the samples calcined at 600–1,000°C are the averages of three cycles obtained from three different electrodes as well. Clearly, the results obtained for the nanofibers calcined at 400°C containing pure anatase phase are much better than those obtained for the nanofibers calcined at 600–1000°C containing mixed anatase-rutile and pure rutile structures. The cyclic stability of the nanofibers calcined at 400°C was evaluated at a discharge rate of 0.3 C. As shown, the nanofibers exhibit a stable cycle life and almost unchanged capabilities after approximately 50 cycles. The Coulombic efficiency at all C rates is at least 96% and almost 100% at higher C-rates. These Coulombic efficiency numbers are much higher than those found for nanofibers reported previously [8–11]. Therefore, an electrode made from binder-free TiO_2 nanofibers possesses acceptable capacity, stable cycling behavior, and acceptable rate performance, showing a promising potential for application as an anode material in lithium-ion batteries, though an optimization of synthesis conditions needs further investigation. Other as-spun nanofibers made from other electrode materials should have been evaluated in order to take the full benefits of the fabrication of nanofibers using the electrospinning method.

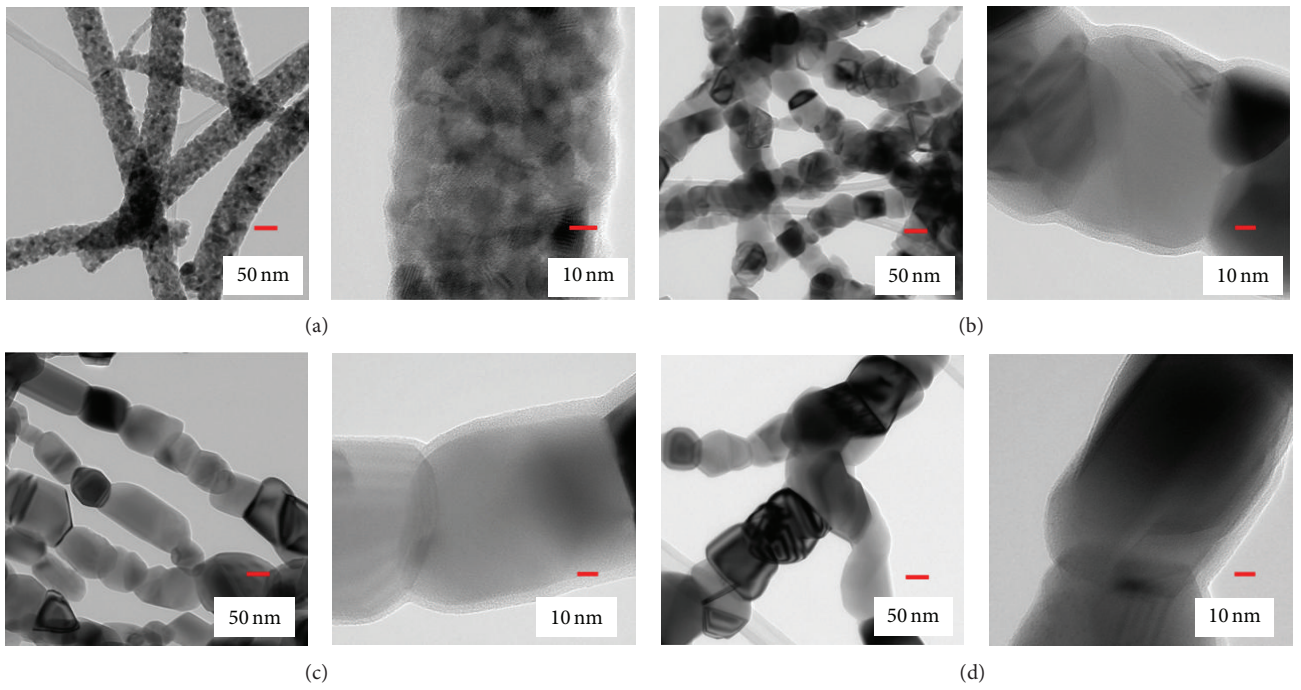

Figure 5: TEM images of carbon-coated TiO_2 nanofibers (a)–(d) calcined in air for 3 h at 400, 600, 800, and 1,000°C, respectively.

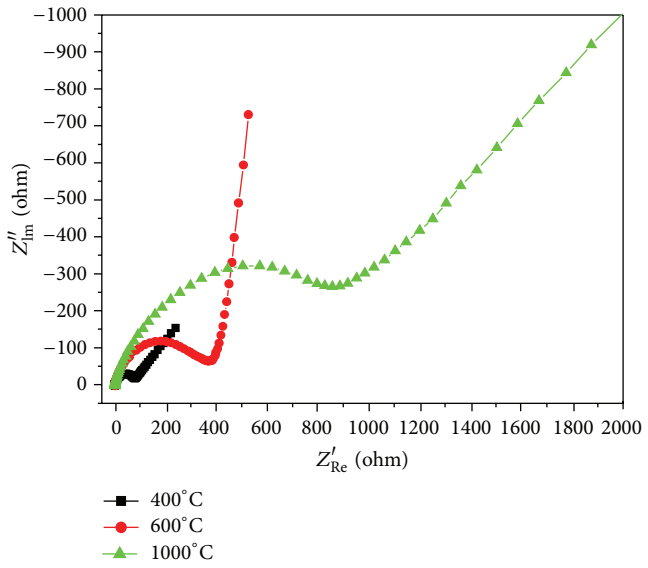

Figure 6: EIS spectra of TiO_2 nanofibers calcined at 400–1,000°C at frequencies ranging from 0.1 to 10^6 Hz.

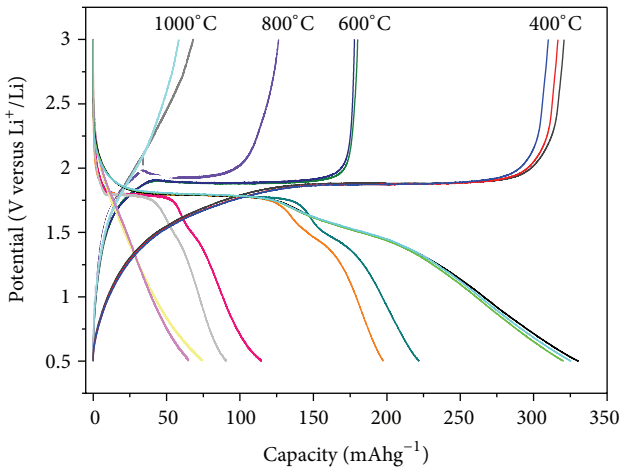

Figure 7: Charge-discharge curves of TiO_2 nanofibers calcined at 400–1,000°C at a current rate of 0.1 C.

4. Conclusions

In this study, TiO_2 nanofibers were prepared using an electrospinning technique. The electrochemical properties of the resulting long and 3D porous fibers were then evaluated directly (as opposed to making composite electrodes) for use as an anode active material in lithium-ion batteries without an additive or a binder. The nanofibers with anatase TiO_2 structure exhibited a high lithium storage capacity, a stable cycle life, and good rate capability, while the nanofibers containing rutile phase show poor performance. The enhanced reversible capacity and cycling performance of the anatase TiO_2 nanofibers are attributed to the large surface area of the nanofibers, small nanocrystallite size, large Li nonstoichiometric parameters (x, y) of TiO_2, and the increased electronic conductivity. This nanofiber material shows promising potential for use as a binder-free anode for rechargeable lithium-ion batteries.

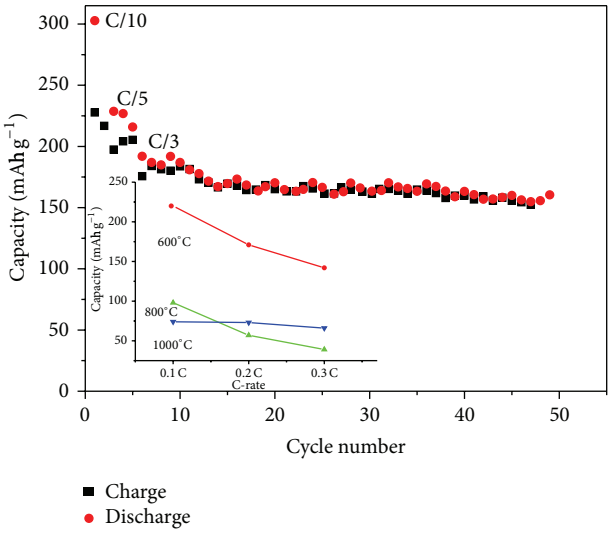

FIGURE 8: Capacity versus cycle number at different current rates of TiO_2 nanofibers calcined at 400°C. Results obtained at 0.1–0.3 C for the samples calcined at 600–1,000°C are also shown (inset).

Conflict of Interests

The authors declare that they have no conflict of interests.

Acknowledgments

This project was financially supported by the Higher Education Research Promotion and National Research University Project of Thailand, Office of the Higher Education Commission through the Advanced Functional Materials Cluster of Khon Kaen University. Nonglak Meethong acknowledges support by the Nanotechnology Center (NANOTEC), NSTDA, Ministry of Science and Technology, Thailand, through its program of Center of Excellence Network.

References

[1] B. L. He, B. Dong, and H. L. Li, "Preparation and electrochemical properties of Ag-modified TiO_2 nanotube anode material for lithium-ion battery," *Electrochemistry Communications*, vol. 9, no. 3, pp. 425–430, 2007.

[2] V. Subramanian, A. Karki, K. I. Gnanasekar, F. P. Eddy, and B. Rambabu, "Nanocrystalline TiO_2 (anatase) for Li-ion batteries," *Journal of Power Sources*, vol. 159, no. 1, pp. 186–192, 2006.

[3] M. A. Reddy, M. S. Kishore, V. Pralong, V. Caignaert, U. V. Varadaraju, and B. Raveau, "Room temperature synthesis and Li insertion into nanocrystalline rutile TiO_2 ," *Electrochemistry Communications*, vol. 8, no. 8, pp. 1299–1303, 2006.

[4] D. V. Bavykin, J. M. Friedrich, and F. C. Walsh, "Protonated titanates and TiO_2 nanostructured materials: synthesis, properties, and applications," *Advanced Materials*, vol. 18, no. 21, pp. 2807–2824, 2006.

[5] H. W. Shim, I. S. Cho, K. S. Hong, W. I. Cho, and D. W. Kim, "Li electroactivity of iron (II) tungstate nanorods," *Nanotechnology*, vol. 21, no. 46, Article ID 465602, 2010.

[6] F. Fang, J. Futter, A. Markwitz, and J. Kennedy, "UV and humidity sensing properties of ZnO nanorods prepared by the arc discharge method," *Nanotechnology*, vol. 20, no. 24, Article ID 245502, 2009.

[7] S. J. Park, Y. J. Kim, and H. Lee, "Synthesis of carbon-coated TiO_2 nanotubes for high-power lithium-ion batteries," *Journal of Power Sources*, vol. 196, no. 11, pp. 5133–5137, 2011.

[8] H. Han, T. Song, J. Y. Bae, L. F. Nazar, H. Kim, and U. Paik, "Nitridated TiO_2 hollow nanofibers as an anode material for high power lithium ion batteries," *Energy & Environmental Science*, vol. 4, pp. 4532–4536, 2011.

[9] Z. Yang, G. Du, Q. Meng et al., "Synthesis of uniform TiO_2@carbon composite nanofibers as anode for lithium ion batteries with enhanced electrochemical performance," *Journal of Materials Chemistry*, vol. 22, pp. 5848–5854, 2012.

[10] X. Zhang, P. S. Kumar, V. Aravindan et al., "Electrospun TiO_2-graphene composite nanofibers as a highly durable insertion anode for lithium ion batteries," *The Journal of Physical Chemistry C*, vol. 116, no. 28, pp. 14780–14788, 2012.

[11] P. Zhu, Y. Wu, M. V. Reddy, A. S. Nair, B. V. R. Chowdari, and S. Ramakrishna, "Long term cycling studies of electrospun TiO_2 nanostructures and their composites with MWCNTs for rechargeable Li-ion batterie," *RSC Advances*, vol. 2, pp. 531–537, 2012.

[12] D. W. Murphy, R. J. Cava, S. M. Zahurak, and A. Santoro, "Ternary Li_xTiO_2 phases from insertion reactions," *Solid State Ionics*, vol. 9-10, no. 1, pp. 413–417, 1983.

[13] R. A. Spurr, "Quantitative analysis of anatase-rutile mixtures with an X-ray diffractometer," *Analytical Chemistry*, vol. 29, no. 5, pp. 760–762, 1957.

[14] W. Nuansing, S. Ninmuang, W. Jarernboon, S. Maensiri, and S. Seraphin, "Structural characterization and morphology of electrospun TiO_2 nanofibers," *Materials Science and Engineering B*, vol. 131, pp. 147–155, 2006.

[15] P. Viswanathamurthi, N. Bhattarai, H. Y. Kim, and D. R. Lee, "Vanadium pentoxide nanofibers by electrospinning," *Scripta Materialia*, vol. 49, no. 6, pp. 577–581, 2003.

[16] S. Maensiri and W. Nuansing, "Thermoelectric oxide $NaCo_2O_4$ nanofibers fabricated by electrospinning," *Materials Chemistry and Physics*, vol. 99, no. 1, pp. 104–108, 2006.

[17] S. Maensiri, W. Nuansing, J. Klinkaewnarong, P. Laokul, and J. Khemprasit, "Nanofibers of barium strontium titanate (BST) by sol-gel processing and electrospinning," *Journal of Colloid and Interface Science*, vol. 297, no. 2, pp. 578–583, 2006.

[18] M. D. Levi and D. Aurbach, "Diffusion coefficients of lithium ions during intercalation into graphite derived from the simultaneous measurements and modeling of electrochemical impedance and potentiostatic intermittent titration characteristics of thin graphite electrodes," *Journal of Physical Chemistry B*, vol. 101, no. 23, pp. 4641–4647, 1997.

[19] M. Wagemaker, W. J. H. Borghols, and F. M. Mulder, "Large impact of particle size on insertion reactions. A case for anatase Li_xTiO_2 ," *Journal of the American Chemical Society*, vol. 129, no. 14, pp. 4323–4327, 2007.

[20] N. Meethong, H. Y. S. Huang, W. C. Carter, and Y. M. Chiang, "Size-dependent lithium miscibility gap in nanoscale $Li_{1-x}FePO_4$," *Electrochemical and Solid-State Letters*, vol. 10, no. 5, pp. A134–A138, 2007.

[21] L. Aldon, P. Kubiak, A. Picard, J. C. Jumas, and J. Olivier-Fourcade, "Size particle effects on lithium insertion into Sn-doped TiO_2 anatase," *Chemistry of Materials*, vol. 18, no. 6, pp. 1401–1406, 2006.

[22] N. Meethong, H. Y. S. Huang, S. A. Speakman, W. C. Carter, and Y. M. Chiang, "Strain accommodation during phase transformations in olivine-based cathodes as a materials selection criterion for high-power rechargeable batteries," *Advanced Functional Materials*, vol. 17, no. 7, pp. 1115–1123, 2007.